

Learning holographic horizons

Vishnu Jejjala,^a Sukrut Mondkar,^{b,c,d} Ayan Mukhopadhyay,^{e,c} Rishi Raj^{c,f}

^a*Mandelstam Institute for Theoretical Physics, School of Physics, NITheCS, and CoE-MaSS, University of the Witwatersrand, Johannesburg, WITS 2050, South Africa*

^b*Harish-Chandra Research Institute, A CI of Homi Bhabha National Institute, Chhatnag Road, Jhansi, Prayagraj (Allahabad) 211019, India*

^c*Center for Strings, Gravitation and Cosmology, Indian Institute of Technology Madras, Chennai 600036, India*

^d*Homi Bhabha National Institute, Training School Complex, Anushakti Nagar, Mumbai 400094, India*

^e*Instituto de Física, Pontificia Universidad Católica de Valparaíso, Avenida Universidad 330, Valparaíso, Chile*

^f*Laboratoire de Physique Théorique et Hautes Energies – LPTHE Sorbonne Université and CNRS, 4 Place Jussieu, 75005 Paris, France*

E-mail: v.jejjala@wits.ac.za, sukrutmondkar@hri.res.in,
ayan.mukhopadhyay@pucv.cl, rishi.raj@lpthe.jussieu.fr

ABSTRACT: We apply machine learning to understand fundamental aspects of holographic duality, specifically the entropies obtained from the apparent and event horizon areas. We show that simple features of only the time series of the pressure anisotropy, namely the values and half-widths of the maxima and minima, the times these are attained, and the times of the first zeroes can predict the areas of the apparent and event horizons in the dual bulk geometry at all times with a fixed maximum length of the input vector. Given that simple Vaidya-type metrics constructed just from the apparent and event horizon areas can be used to approximately obtain unequal time correlation functions, we argue that the corresponding entropy functions are the information that can be learnt from a single one-point function (without explicit knowledge of the gravitational dynamics) and that is necessary for reconstructing specific aspects of the dual quantum state to the best possible approximations.

Contents

1	Introduction	1
2	Holographic setup	3
2.1	Event and apparent horizons	5
3	Machine learning entropy	6
4	Discussion and outlook	8
A	Feedforward neural networks	11
B	Data preparation and analysis	12

1 Introduction

The central idea behind modern approaches to Big Data is to devise a predictive analytics by isolating and focusing on salient features within a large dataset. Often, we do not know what the important features are *a priori*. Machine learning can be successful at identifying subtle correlations within datasets and extracting relationships in order to make testable predictions. Unboxing an effective machine learning architecture may in fact teach us about the structure of data.

Spacetime is Big Data. Moreover, in certain settings, we have prior access to the most efficient data compression protocol available for encoding a dataset. This is holography [1, 2]. The gauge/gravity correspondence in asymptotically anti-de Sitter (AdS) spaces [3–5] and the Matrix model for M-theory [6] supply examples where the degrees of freedom of a gravitational system are explicitly codimension one. In this respect, the fundamental understanding of the emergence of semiclassical spacetime

from a strongly coupled gauge theory living at the boundary is also one of the prominent areas of interdisciplinary research in theoretical physics (see [7, 8] for reviews).

To date, there have been few investigations of the holographic correspondence in the context of machine learning [9–15]. The subject of this letter is to demonstrate that features of the bulk geometry can be machine learned from information contained purely within the dual quantum field theory. In particular, we address the notion of the entropies associated with the dynamical horizons of the emergent geometry corresponding to a typical non-equilibrium state in the dual field theory. This can be expected to provide new insights into some fundamental aspects of the holographic duality since the horizons are among the important gauge invariant features of a spacetime, and the physical understanding of the non-equilibrium entropies associated with the horizons should have important consequences for our understanding of the emergence of spacetime.

In the language of numerical general relativity, the problem is the following. We set initial conditions for a four-dimensional asymptotically anti-de Sitter (aAdS₄) geometry which satisfies the vacuum Einstein equation with a negative cosmological constant. The resulting solution of the gravitational equations is dual to a non-equilibrium state which eventually thermalizes, mirroring the ubiquitous feature of gravity that any spacetime eventually settles down to a static AdS₄–Schwarzschild black hole. The irreversibility is captured by the growth of the areas of the apparent and event horizons that ultimately coincide, and these give two non-equilibrium entropy functions. From the asymptotic behaviour of the aAdS₄ metric, one can read off the (time dependent) energy-momentum tensor in the dual theory, particularly the pressure anisotropy [16, 17]. In principle, with the latter data we can reconstruct the dual spacetime and thus the entropies. Here, we study whether we can use machine learning to reconstruct the apparent and event horizon areas from simple features of the time series of the pressure anisotropy.

This problem is of interest because it has been shown earlier that just with the data of the time dependent event and apparent horizon areas one can explicitly construct simple spacetime metrics of AdS–Vaidya type [18, 19] which do not satisfy the Einstein equations but give excellent approximations to many other observables in the dual field

theory such as correlation functions.¹ Therefore, deducing the growth of the entropies from simple features of the time series of pressure anisotropy can lead us to predict other features of the dual state in holographic theories, especially correlation functions of various operators, simplifying numerical holography and opening the door to new insights not only into the dynamics of strongly coupled quantum many-body systems but also into the fundamental nature of the holographic duality as discussed in the concluding section.

2 Holographic setup

In the limit of strong coupling and large rank of the gauge group, holography maps the non-equilibrium dynamics of quantum field theories to classical gravitational dynamics in asymptotically anti-de Sitter (AdS) spacetimes in one higher spatial dimension [3–5]. In this section, we describe the setup of the dual gravitational problem, which will subsequently be used to generate data for our machine learning task. To do this, we solve the Einstein equations starting from a non-equilibrium asymptotically AdS metric, which represents the out-of-equilibrium initial state of the dual field theory. (See [20, 21] for some excellent reviews on this topic.) By holographic renormalization [16, 17, 22], we obtain the expression for the stress tensor of the dual quantum theory. The bulk metric settles down eventually to a planar AdS–Schwarzschild black hole which is dual to the finite temperature state in the gauge theory. We obtain the entropies by locating the event and apparent horizons in the numerically obtained bulk metrics and computing their time dependent areas.

A typical homogeneous metric of an asymptotically AdS₄ black brane in Eddington–Finkelstein coordinates (with flat Minkowski metric on the boundary) is

$$ds^2 = 2 dr dt - A(r, t) dt^2 + S(r, t)^2 (e^{-B(r, t)} dx^2 + e^{B(r, t)} dy^2) , \quad (2.1)$$

where r is the bulk radial coordinate (the boundary of spacetime is at $r \rightarrow \infty$), t is time coordinate on the boundary, which is a null coordinate in the bulk, and x and y are boundary spatial coordinates. In what follows, we will denote the bulk coordinates by

¹An AdS–Vaidya metric has a single non-trivial function namely a mass which is a function of the boundary (field theory) coordinates. An analogue construction is a thermal density matrix with a spacetime dependent temperature. However, the latter is not equivalent to an AdS–Vaidya metric which is more natural in holography from the point of view of the emergent bulk geometry.

capital Latin indices and boundary coordinates by Greek indices. The metric is written in terms of A , B , and S , which are functions of the radial coordinate and time. We focus on AdS₄ as this supplies the simplest examples; it is straightforward to generalize to higher dimensions.

A special case of (2.1) is the Schwarzschild–AdS₄ black brane metric for which

$$A(r, t) = \frac{r^2}{L^2} - \frac{ML^2}{r}, \quad B(r, t) = 0, \quad S(r, t) = \frac{r}{L}, \quad (2.2)$$

where M is the ADM mass [23], which is related to Hawking temperature T by the relation

$$M = \frac{64}{27} L^3 \pi^3 T^3, \quad (2.3)$$

with L being the radius of AdS₄. The event and apparent horizons coincide at the position $r_{\text{H}} = L^{4/3} M^{1/3}$. We will use units in which $L = 1$ since only dimensionless combinations with L relate to physical constants and variables in the dual three dimensional conformal field theory.

The boundary metric is identified with the physical background metric on which the dual field theory lives. Requiring that it is a codimension one Minkowski space, implies that the functions A , B , and S should behave as follows

$$A(r, t) = r^2 + \frac{a_n(t)}{r} + \dots, \quad B(r, t) = \frac{b_n(t)}{r^3} + \dots, \quad S(r, t) = r - \frac{1}{8r} + \dots, \quad (2.4)$$

at large r . The normalizable modes $a_n(t)$ and $b_n(t)$ give the energy density (ϵ) and the pressure anisotropy ($P_x - P_y$) in the dual state, respectively [16, 17]. Explicitly, the expectation value of the dual energy-momentum tensor $T^{\mu\nu}$ obtained from holographic renormalization has the following non-vanishing components

$$\hat{T}^{tt} = \hat{\epsilon} = -2a_n(t), \quad \hat{T}^{xx} = \hat{P}_x = -a_n(t) - 3b_n(t), \quad \hat{T}^{yy} = \hat{P}_y = -a_n(t) + 3b_n(t), \quad (2.5)$$

where $\hat{T}^{\mu\nu}$ is defined via $T^{\mu\nu} = \kappa^{-1} \hat{T}^{\mu\nu}$ with $\kappa^{-1} = (8\pi G_N)^{-1}$ (in units $L = 1$ and G_N being Newton's gravitational constant) identified with N^2 up to a numerical constant. As expected in a conformal field theory, the energy-momentum tensor is traceless. The functions $a_n(t)$ and $b_n(t)$ are determined by the initial conditions for the bulk metric as discussed below.

The bulk Einstein equations in the characteristic form are [20]:

$$\begin{aligned} S'' &= -\frac{1}{4} S (B')^2, & \dot{S}' &= \frac{3S}{2} - \frac{\dot{S}S'}{S}, \\ \dot{B}' &= -\frac{\dot{S}B'}{S} - \frac{\dot{B}S'}{S}, & A'' &= \frac{4\dot{S}S'}{S^2} - \dot{B}B', & \dot{S} &= \frac{\dot{S}A'}{2} - \frac{\dot{B}^2 S}{4}. \end{aligned} \quad (2.6)$$

Above, the prime denotes the radial derivative, and the dot denotes the derivative along the outgoing null geodesic, *e.g.*,

$$\dot{f}(r, t) := \partial_t f + \frac{A(r, t)}{2} f'(r, t) . \quad (2.7)$$

The first four expressions in (2.6) are *radial* evolution equations which are solved for the functions S , \dot{S} , \dot{B} and A in this order at every time step. The last equation for \ddot{S} is a constraint equation implying the conservation of the dual energy-momentum tensor (2.5) in background Minkowski metric. The latter simply states that $a_n(t)$ is a constant. It should be obvious from the nested characteristic form of the gravitational equations that given the radial profile of B (*i.e.*, $B(r, t = 0)$) at an initial time and the initial value of a_n (which turns out to be a constant), we obtain unique solutions for $S(r, t)$, $B(r, t)$ and $A(r, t)$ satisfying the asymptotic behavior (2.4), and thus a unique bulk metric. The necessary time updates of the radial profile of S and B (by using \dot{S} and \dot{B} , respectively) are done via the fourth order Adams–Bashforth method. The constraint equation evaluated at several radial locations can be used to monitor the accuracy of numerics. See Appendix B for more details.²

2.1 Event and apparent horizons

In thermal equilibrium, the entropy of the dual field theory is calculated from the area of the event horizon via the Bekenstein–Hawking formula: $S = \frac{A_{\text{EH}}}{4G}$. However, in out-of-equilibrium settings, the entropy in the dual field theory can be given by the area of the apparent horizon, which is the outermost trapped surface [24–26]. The area of the event horizon, which satisfies the second law strictly [27, 28], enumerates the spacetime degrees of freedom.³ The apparent horizon is always interior to (or coincident with) the event horizon. As well, the apparent horizon is defined locally on a given spacelike slice, whereas the event horizon is a global property of the spacetime, and therefore harder to compute.

²For the purpose of numerics, it is useful to further redefine variables and take advantage of a residual gauge freedom. The domain of the radial coordinate is typically set to $r \geq r_0$ such that it includes the apparent and thus the event horizon.

³A generalized second law can be argued to hold for general null congruences [29, 30].

The position of the event horizon (r_{EH}) is obtained from the solution to the equation [21]

$$\frac{d}{dt}r_{\text{EH}}(t) - \frac{A(r_{\text{EH}}(t), t)}{2} = 0 , \quad (2.8)$$

subject to the boundary condition $r_{\text{EH}}(t \rightarrow \infty) = M_f^{1/3}$, where M_f is the ADM mass of the *final* equilibrated black brane. The position of the apparent horizon (r_{AH}) is determined by solving the algebraic equation [21]

$$\dot{S}(r_{\text{AH}}, t) = 0 . \quad (2.9)$$

The entropy density of the dual field theory system, which is proportional to the area of either the event or the apparent horizons as appropriate, is given by

$$s_*(t) = \frac{1}{2\pi} S(r_*(t), t)^2 . \quad (2.10)$$

In the numerical code, we use the variable $z = \frac{1}{r}$ instead of r for the radial bulk coordinate since z has finite range unlike r .

We can use various initial conditions given by $B(z, t = 0)$ and $a_n(t = 0)$ and solve the Einstein equations. (Recall that $a_n(t)$ turns out to be a constant.) Thus we obtain the boundary anisotropy $b_n(t)$ time series data. Since the dual conformal field theory has no intrinsic scale, we can set $a_n = -1$ so that the dual energy density is given by $\hat{\epsilon} = 2$ without any loss of generality. We design the neural network to predict the areas of the event and apparent horizons (at all times) from this boundary anisotropy time series data.

3 Machine learning entropy

To predict the areas of event and apparent horizons, we employ *deep neural networks*. (We briefly summarize neural networks in Appendix A. See [31, 32] for excellent contemporary reviews.) The training data for these predictions are the time series for the boundary pressure anisotropy, $b_n(t)$.

We use various initial conditions for $B(z, t = 0)$ by holding the energy density fixed (in the appropriate units) to 2. This corresponds to choosing the initial condition $a_n(t = 0) = -1$. This ensures that all the initial conditions in the dataset thermalize at approximately the same time (because energy or equivalently the temperature sets

the timescale of thermalization $t_{\text{th}} \approx 2$). We find that the learning of event horizon as well as apparent horizon areas happens almost perfectly at all times from the initial time until the time at which the system thermalizes.

Our main result is that training the neural network with only a handful of simple features of $b_n(t)$ time series suffices to generate predictions comparable to the predictions made by the neural network trained on the full $b_n(t)$ time series data. These simple features involve just the maximum and minimum values of the pressure anisotropy and the respective times when they are attained, the half width of the maxima and the minima, and the zeroes of the time series truncated at $t = 3$. This data with such *short input vectors* restricted to a maximum length of 100 (by truncating the last set of zeroes if needed) predicts both the event and apparent horizon areas (almost) perfectly at all times.⁴ It is to be noted that although the apparent horizon is determined causally unlike the event horizon, as should be obvious from our previous discussion, for the short input vector we should include data from times beyond the time at which the apparent horizon is being predicted simply because we are sparsifying the past data.

The details of the machine learning computation are given in Appendix B along with a statistical analysis of the results. Figure 1 gives representative plots.

⁴For $t > t_{\text{th}}$, the event and apparent horizons approximately coincide (representing thermalization in the dual theory) and their areas are determined given just by the conserved energy. For $t < t_{\text{th}}$, more data are necessary. $t_{\text{th}} \approx 2$ is the common thermalization time for our dataset.

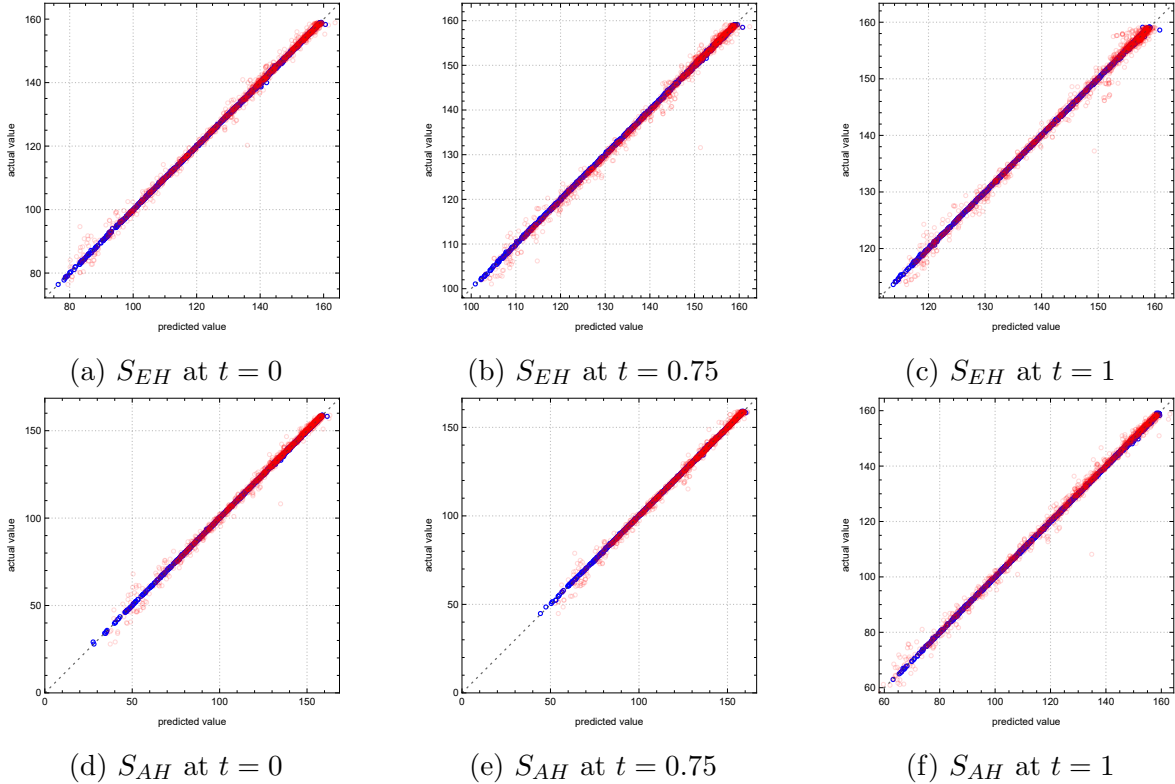


Figure 1: Testing statistics for S_{EH} and S_{AH} with both **long input vector** (blue) as well as **short input vector** (red) at various times. Note that the scale is set by the (conserved) energy density which is the same for all the elements of the dataset used for machine learning, which makes it meaningful to compare the times across the dataset.

4 Discussion and outlook

In this letter, we have demonstrated that neural networks can learn some aspects of bulk geometry given simply the time series of a one-point function (expectation value of an operator) as input. In particular, we establish that the areas of the event and apparent horizons can be learned from the time series data of the pressure anisotropy in the boundary field theory. Furthermore, neural networks also predict the black hole entropies at all times from only a small number of features of the time series data, namely the values and half-widths of the maxima and minima, the times the latter are attained, and the times of the first zeroes with the maximum length of the input vector

set to 100 and the time series truncated to a maximum value of time commensurate with the thermalization time. This is surprising and points to universality classes of bulk metrics and their dual states which can be characterized only by simple features of the time series of a simple observable. Our work therefore indicates that neural networks are a promising tool for addressing bulk reconstruction in AdS/CFT and obtaining new insights into holographic dynamics.

Our work can also pave the way to a more fundamental understanding of the holographic duality especially with respect to the microscopic understanding of the meaning of the entropies captured by the areas of the apparent and event horizons. Since the AdS-Vaidya metrics have only one non-trivial function of the boundary (field theory) coordinates, namely the effective mass (temperature), they are gravitational analogs of maximum entropy ensembles. Given that one can construct simple aAdS₄-Vaidya metrics based on the time series of the apparent and event horizon entropies, and obtain excellent approximations to correlations functions [19], we can speculate that these entropy functions provide the keys to construct simple approximations to the non-equilibrium quantum state just from simple features of a one-point function such that it allows us to deduce even complex observables including time dependent correlation functions with sufficiently good approximation. Existence of such entropy functions are not generally guaranteed but our present results together with the observations of [18, 19] indicate their existence in a large- N holographic quantum field theory. In particular, aAdS₄-Vaidya metric which matches the apparent horizon area of the actual geometry at all times give excellent approximations to correlations for arbitrary values of the two time arguments while that based on the event horizon area give better approximations to the correlations in the regime where the correlations depend on the conserved energy and the effective transition time [19].⁵

⁵In [19], various AdS-Vaidya geometries with only a time dependent effective mass were constructed such that different physical quantities match the exact numerical geometry at all times. The numerical geometry was generated by sourcing a bulk scalar field minimally coupled to gravity, It was found that the AdS-Vaidya geometry that matched the apparent horizon area of the actual solution at all times gave the best approximation to the two-point correlations for arbitrary values of the two time arguments, whereas the one which matched the event horizon area at all times gave the best approximation to the correlations in a regime where they depended only on the initial and final temperatures and the effective time duration of the pump which drives the non-equilibrium transition (for the retarded correlation function it meant that the observation time was away from the time when the pump was maximally strong). To compare with our present case, we can simply take a time slice

Therefore, *the entropy function obtained from the apparent horizon can be interpreted as the information which can be learnt just from a single one-point function and which is necessary to reconstruct correlation functions to the best possible approximation.* This learning can be achieved without explicit knowledge of the dual gravitational dynamics. *Similarly, the entropy function based on the event horizon area is the information that can be extracted from the one-point function and needed to reconstruct aspects of the correlations which depend only on the energy, and the strength and duration of the drive needed to prepare the non-equilibrium state.* Machine learning could be a powerful tool for validating and further developing the statistical understanding of the entropy functions associated with the dynamical horizons in holographic theories. *Diversifying the training by going beyond the pure gravity setup explored here, we need to verify if the event and apparent horizon areas can be predicted from the pressure anisotropy data without explicit knowledge of the gravitational equations.* Furthermore, it would be interesting to explore if such entropy functions can exist generally in large- N field theories. It should be interesting to note that our discussion has resemblances with interpretations of emergent spacetimes in terms of statistical ensembles, as for instance that advocated in [33].

In the future, we would like to unbox the neural network in order to understand how learning takes place, for instance, by employing techniques like layer-wise relevance propagation [34, 35] and this should be important for the stated goal of interpreting the entropy functions. Because this work is a proof of principle that we can apply Big Data techniques to holography and machine learn salient features of spacetime dynamics from dual data, we do not have a need to optimize the network hyperparameters to improve performance. It would be good to do this, of course.

Acknowledgements

We are grateful to Jessica Craven, Koji Hashimoto, Shivaprasad Hulyal, Arjun Kar, and Tanay Kibe for enlightening discussions on this and related work. We acknowledge the High-Performance Scientific Computing facility of the Harish-Chandra Research Institute, where we generated most of the data used for training and testing our neural

where the source (and the scalar field) has decayed but the geometry is still out of equilibrium so that we can approximate the subsequent evolution by pure gravity. For a more precise understanding, we should put in an explicit source. We plan to do so in the future.

networks. We thank the organizers and participants of String Data 2022, where aspects of this work were presented. VJ is supported by the South African Research Chairs Initiative of the Department of Science and Innovation and the National Research Foundation. VJ would as well like to thank the Isaac Newton Institute for Mathematical Sciences for support and hospitality during the program “Black holes: bridges between number theory and holographic quantum information” during which work on this paper transpired; this work was supported by EPSRC grant number EP/R014604/1. The research of AM was partly supported by the center of excellence grants of the Ministry of Education of India.

A Feedforward neural networks

Consider the map

$$\begin{aligned} f_i : \mathbb{R}^{n_{i-1}} &\rightarrow \mathbb{R}^{n_i} \\ \mathbf{v}_{i-1} &\mapsto \mathbf{v}_i = \sigma(\mathbf{v}'_i) \end{aligned} \quad (\text{A.1})$$

where $\mathbf{v}'_i = W^{(i)} \cdot \mathbf{v}_{i-1} + \mathbf{b}_i$. The vector $\mathbf{b}_i \in \mathbb{R}^{n_i}$ is called a *bias vector* and the $n_i \times n_{i-1}$ matrix $W^{(i)}$ is called a *weight matrix*. The *activation function* σ acts non-linearly elementwise on the components of the vector \mathbf{v}'_i . In our case, we choose $\sigma(x) = x \Theta(x)$, where $\Theta(x)$ is the Heaviside step function. (This is the rectified linear unit or ReLU activation.) Taking the vector $\mathbf{v}_{\text{in}} := \mathbf{v}_0 \in \mathbb{R}^{n_0}$ as the input vector, this procedure is iterated:

$$\mathbf{v}_\ell = f_\ell(f_{\ell-1}(\cdots(f_1(\mathbf{v}_0)\cdots))) \ , \quad a_{\text{out}} := \sum_{m=1}^{n_\ell} \mathbf{v}_\ell^m \ . \quad (\text{A.2})$$

In writing a_{out} , we have summed the components of the vector \mathbf{v}_ℓ .

Suppose we have a set of input vectors labeled by j that we use for training. To each of these input vectors $\mathbf{v}_{\text{in},j}$ we associate a target value $\alpha_j \in \mathbb{R}$. We then consider a mean squared loss function that compares each α_j to its predicted value $a_{\text{out},j}$. Backpropagation enables us to tune the elements of the weight matrices and bias vectors to minimize this loss. In this way, we have constructed an ℓ -hidden layer fully connected feedforward neural network that is trained to approximate α_j from the features encoded in $\mathbf{v}_{\text{in},j}$ via stochastic gradient descent. The dimension n_i specifies the number of neurons in the i -th hidden layer.

In our experiments, the architectures of the neural network are dependent on the vector \mathbf{v}_{in} . With long input vectors in \mathbb{R}^{299} , we use three hidden layers with 2000 neurons each. With short input vectors in \mathbb{R}^{100} , we use three hidden layers with 150 neurons each. (The input vectors are described in Appendix B.) We use 70% of a 10000 data points for training, 15% for validation, and 15% for testing. Performance statistics are reported on the test set. The neural networks are implemented in `Mathematica` [36] and use `Adam` for optimization. We make our code available on `GitHub` [37].

B Data preparation and analysis

We use the following family of profiles for specifying the initial conditions of $B(z, t = 0)$:

$$B(z, t = 0) = z^3 \left(\mathcal{R}_1 e^{-200(z-0.2)^2} + \mathcal{R}_2 e^{-200(z-0.5)^2} \mathcal{R}_3 e^{-100(z-0.8)^2} \right), \quad (\text{B.1})$$

where $\mathcal{R}_{1,2,3}$ are (pseudo)random numbers between 0 and 1 and $z = L^2/r$. These profiles are superpositions of three Gaussians centered at 0.2, 0.5, and 0.8, respectively. (The range of bulk radial coordinate z is between 0 and 1 which includes the apparent horizon (and thus the event horizon as well) as we set $L = 1$ and $a_n = -1$.) By varying $\mathcal{R}_{1,2,3}$, we generate various initial conditions. We use the characteristic method outlined in the main text to solve the Einstein equations wherein at each time step, a set of nested ordinary differential equations in radial coordinate r (or equivalently z) are solved using the pseudospectral method [20, 38]. In the pseudospectral method, the radial coordinate r is discretized using a Chebyshev grid with a certain choice of the number of grid points, n . In our simulations, we have chosen $n = 60$. The time updates are performed using the 4th order Adams–Bashforth method (see main text). This method requires knowing the values of the functions to be time evolved at previous four time steps. Therefore, for the first nine time steps, we use smaller time steps and perform numerical integration of the interpolated functions. From the 10th time step onwards, the 4th order Adams–Bashforth method is used for time stepping with the value of time step $\delta t = 0.001$. The residual gauge freedom in (2.1) is fixed by setting the coefficient of r in the near-boundary expansion of $A(r, t)$ in (2.4) to zero.

As described in the main text, we employ neural networks to make predictions of the areas of the event and the apparent horizons at various times. We observe that the (common) thermalization time (t_{th}) is approximately equal to 2 (set by the energy density, *i.e.*, a_n), so we choose $t = 0, 0.75$, and 1 as representative values. In each case,

we train the neural network on the longer $b_n(t)$ time series data (referred to as a *long input vector*) as well as on the shorter data which retains only a handful of features of $b_n(t)$ time series data (referred to as a *short input vector*). More precisely, the long input vector is $b_n(t_0 + k\delta t)$, where $\delta t = 0.01$ and

$$k = (10^{-4}, 10^{-7/2}, 10^{-3}, 10^{-5/2}, 10^{-2}, 10^{-3/2}, 10^{-1}, 10^{-1/2}, 1 - \sum_{i=-8}^{-1} 10^{i/2})$$

for first nine time steps respectively and $k = 1$ from 10th time step onward. (Although, we use time step $\delta t = 0.001$ for the simulations that generate elements of our dataset, for the long input vector, we only keep values of various dynamical quantities with $\delta t = 0.01$.) The full time series is truncated to $t = 3$.

A *short input vector* contains a certain handful of features of the pressure anisotropy time series. The features of interest are:

1. $b_{n,\max}$: maximum value that $b_n(t)$ takes;
2. t_{\max} : time t when $b_{n,\max}$ is attained;
3. $b_{n,\min}$: minimum value that $b_n(t)$ takes;
4. t_{\min} : time t when $b_{n,\min}$ is attained;
5. full width at half maximum;
6. full width at half minimum ;
7. times corresponding to the zeroes of $b_n(t)$.

Note that the number of zeros of $b_n(t)$ is in general different for different initial conditions. Therefore we fix the maximum length of the input vector to 100 by padding with zeroes on the right as necessary. Note also that the full time series is truncated to $t = 3$.

To assess the performance of the neural network, we compute the following quantities over the test set:

$$\text{mean deviation (MD)} : \text{Mean}\left[\frac{\text{Abs}[\text{actual} - \text{predicted}]}{\text{actual}}\right], \quad (\text{B.2})$$

$$\text{baseline} : \text{Mean}\left[\frac{\text{Abs}[\text{actual} - \text{Mean}[\text{actual}]]}{\text{actual}}\right]. \quad (\text{B.3})$$

The baseline (B.3) simply assigns the mean in the dataset as a universal prediction. The accuracy of the trained neural network is compared to this baseline. We as well calculate the standard deviation (SD) between the actual value and the predicted value, R -squared, and χ -squared in the usual way. These statistics are reported in Tables 1 and 2.

time	input vector	MD	baseline	SD	R -squared	χ -Squared
$t = 0$	long	0.00126523	0.146794	0.226	1.00	0.579892
	short	0.0055714	0.146794	1.20	0.997	18.8811
$t = 0.75$	long	0.000825361	0.101556	0.161	1.00	0.273529
	short	0.00471945	0.101556	1.11	0.995	14.2559
$t = 1$	long	0.000615757	0.0820156	0.132	1.00	0.173059
	short	0.00400621	0.0820156	0.132	1.00	9.79269

Table 1: Various statistical measures assessing performance of neural network for S_{EH} prediction.

time	input vector	MD	baseline	SD	R -squared	χ -Squared
$t = 0$	long	0.00153455	0.249098	0.251	1.00	0.855986
	short	0.0116055	0.249098	1.92	0.996	74.8623
$t = 0.75$	long	0.00155447	0.197801	0.245	1.00	0.782011
	short	0.00885326	0.197801	1.64	0.996	45.6544
$t = 1$	long	0.00132608	0.18089	0.220	1.00	0.574205
	short	0.00776989	0.18089	1.68	0.995	40.2655

Table 2: Various statistical measures assessing performance of neural network for S_{AH} prediction.

References

- [1] G. 't Hooft, Dimensional reduction in quantum gravity, Conf. Proc. C 930308 (1993) 284–296. [arXiv:gr-qc/9310026](https://arxiv.org/abs/gr-qc/9310026).
- [2] L. Susskind, The World as a hologram, J. Math. Phys. 36 (1995) 6377–6396. [arXiv:hep-th/9409089](https://arxiv.org/abs/hep-th/9409089), [doi:10.1063/1.531249](https://doi.org/10.1063/1.531249).

- [3] J. M. Maldacena, The Large N limit of superconformal field theories and supergravity, *Adv. Theor. Math. Phys.* 2 (1998) 231–252. [arXiv:hep-th/9711200](#), [doi:10.4310/ATMP.1998.v2.n2.a1](#).
- [4] S. S. Gubser, I. R. Klebanov, A. M. Polyakov, Gauge theory correlators from noncritical string theory, *Phys. Lett. B* 428 (1998) 105–114. [arXiv:hep-th/9802109](#), [doi:10.1016/S0370-2693\(98\)00377-3](#).
- [5] E. Witten, Anti-de Sitter space and holography, *Adv. Theor. Math. Phys.* 2 (1998) 253–291. [arXiv:hep-th/9802150](#), [doi:10.4310/ATMP.1998.v2.n2.a2](#).
- [6] T. Banks, W. Fischler, S. H. Shenker, L. Susskind, M theory as a matrix model: A Conjecture, *Phys. Rev. D* 55 (1997) 5112–5128. [arXiv:hep-th/9610043](#), [doi:10.1103/PhysRevD.55.5112](#).
- [7] D. Harlow, TASI Lectures on the Emergence of Bulk Physics in AdS/CFT, *PoS TASI2017* (2018) 002. [arXiv:1802.01040](#), [doi:10.22323/1.305.0002](#).
- [8] T. Kibe, P. Mandayam, A. Mukhopadhyay, Holographic spacetime, black holes and quantum error correcting codes: a review, *Eur. Phys. J. C* 82 (5) (2022) 463. [arXiv:2110.14669](#), [doi:10.1140/epjc/s10052-022-10382-1](#).
- [9] K. Hashimoto, AdS/CFT correspondence as a deep Boltzmann machine, *Phys. Rev. D* 99 (10) (2019) 106017. [arXiv:1903.04951](#), [doi:10.1103/PhysRevD.99.106017](#).
- [10] H.-Y. Hu, S.-H. Li, L. Wang, Y.-Z. You, Machine Learning Holographic Mapping by Neural Network Renormalization Group, *Phys. Rev. Res.* 2 (2) (2020) 023369. [arXiv:1903.00804](#), [doi:10.1103/PhysRevResearch.2.023369](#).
- [11] Y.-K. Yan, S.-F. Wu, X.-H. Ge, Y. Tian, Deep learning black hole metrics from shear viscosity, *Phys. Rev. D* 102 (10) (2020) 101902. [arXiv:2004.12112](#), [doi:10.1103/PhysRevD.102.101902](#).
- [12] K. Hashimoto, R. Watanabe, Bulk reconstruction of metrics inside black holes by complexity, *JHEP* 09 (2021) 165. [arXiv:2103.13186](#), [doi:10.1007/JHEP09\(2021\)165](#).
- [13] K. Li, Y. Ling, P. Liu, M.-H. Wu, Learning the black hole metric from holographic conductivity, *Phys. Rev. D* 107 (6) (2023) 066021. [arXiv:2209.05203](#), [doi:10.1103/PhysRevD.107.066021](#).
- [14] J. Craven, V. Jejjala, A. Kar, Calculating out-of-time-ordered correlation functions in the SYK model using machine learning, presented at String Data 2022.

- [15] P. Kumar, T. Mandal, S. Mondal, Black Holes and the loss landscape in machine learning, JHEP 10 (2023) 107. [arXiv:2306.14817](#), [doi:10.1007/JHEP10\(2023\)107](#).
- [16] V. Balasubramanian, P. Kraus, A Stress tensor for Anti-de Sitter gravity, Commun. Math. Phys. 208 (1999) 413–428. [arXiv:hep-th/9902121](#), [doi:10.1007/s002200050764](#).
- [17] S. de Haro, S. N. Solodukhin, K. Skenderis, Holographic reconstruction of space-time and renormalization in the AdS / CFT correspondence, Commun. Math. Phys. 217 (2001) 595–622. [arXiv:hep-th/0002230](#), [doi:10.1007/s002200100381](#).
- [18] S. Bhattacharyya, S. Minwalla, Weak Field Black Hole Formation in Asymptotically AdS Spacetimes, JHEP 09 (2009) 034. [arXiv:0904.0464](#), [doi:10.1088/1126-6708/2009/09/034](#).
- [19] L. K. Joshi, A. Mukhopadhyay, F. Preis, P. Ramadevi, Exact time dependence of causal correlations and nonequilibrium density matrices in holographic systems, Phys. Rev. D 96 (10) (2017) 106006. [arXiv:1704.02936](#), [doi:10.1103/PhysRevD.96.106006](#).
- [20] P. M. Chesler, L. G. Yaffe, Numerical solution of gravitational dynamics in asymptotically anti-de Sitter spacetimes, JHEP 07 (2014) 086. [arXiv:1309.1439](#), [doi:10.1007/JHEP07\(2014\)086](#).
- [21] W. van der Schee, Gravitational collisions and the quark-gluon plasma, Ph.D. thesis, Utrecht U. (2014). [arXiv:1407.1849](#).
- [22] K. Skenderis, Lecture notes on holographic renormalization, Class. Quant. Grav. 19 (2002) 5849–5876. [arXiv:hep-th/0209067](#), [doi:10.1088/0264-9381/19/22/306](#).
- [23] R. L. Arnowitt, S. Deser, C. W. Misner, Dynamical Structure and Definition of Energy in General Relativity, Phys. Rev. 116 (1959) 1322–1330. [doi:10.1103/PhysRev.116.1322](#).
- [24] P. M. Chesler, L. G. Yaffe, Horizon formation and far-from-equilibrium isotropization in supersymmetric Yang-Mills plasma, Phys. Rev. Lett. 102 (2009) 211601. [arXiv:0812.2053](#), [doi:10.1103/PhysRevLett.102.211601](#).
- [25] I. Booth, M. P. Heller, G. Plewa, M. Spalinski, On the apparent horizon in fluid-gravity duality, Phys. Rev. D 83 (2011) 106005. [arXiv:1102.2885](#), [doi:10.1103/PhysRevD.83.106005](#).
- [26] N. Engelhardt, A. C. Wall, Decoding the Apparent Horizon: Coarse-Grained Holographic Entropy, Phys. Rev. Lett. 121 (21) (2018) 211301. [arXiv:1706.02038](#), [doi:10.1103/PhysRevLett.121.211301](#).

- [27] S. W. Hawking, Gravitational radiation from colliding black holes, *Phys. Rev. Lett.* 26 (1971) 1344–1346. doi:[10.1103/PhysRevLett.26.1344](https://doi.org/10.1103/PhysRevLett.26.1344).
- [28] R. M. Wald, The thermodynamics of black holes, *Living Rev. Rel.* 4 (2001) 6. [arXiv:gr-qc/9912119](https://arxiv.org/abs/gr-qc/9912119), doi:[10.12942/lrr-2001-6](https://doi.org/10.12942/lrr-2001-6).
- [29] R. Bousso, A Covariant entropy conjecture, *JHEP* 07 (1999) 004. [arXiv:hep-th/9905177](https://arxiv.org/abs/hep-th/9905177), doi:[10.1088/1126-6708/1999/07/004](https://doi.org/10.1088/1126-6708/1999/07/004).
- [30] R. Bousso, Z. Fisher, S. Leichenauer, A. C. Wall, Quantum focusing conjecture, *Phys. Rev. D* 93 (6) (2016) 064044. [arXiv:1506.02669](https://arxiv.org/abs/1506.02669), doi:[10.1103/PhysRevD.93.064044](https://doi.org/10.1103/PhysRevD.93.064044).
- [31] P. Mehta, M. Bukov, C.-H. Wang, A. G. Day, C. Richardson, C. K. Fisher, D. J. Schwab, [A high-bias, low-variance introduction to machine learning for physicists](https://arxiv.org/abs/1903.08237), *Physics Reports* 810 (2019) 1–124. doi:[10.1016/j.physrep.2019.03.001](https://doi.org/10.1016/j.physrep.2019.03.001). URL <https://doi.org/10.1016%2Fj.physrep.2019.03.001>
- [32] F. Ruehle, Data science applications to string theory, *Phys. Rept.* 839 (2020) 1–117. doi:[10.1016/j.physrep.2019.09.005](https://doi.org/10.1016/j.physrep.2019.09.005).
- [33] D. L. Jafferis, D. K. Kolchmeyer, B. Mukhametzhanov, J. Sonner, Jackiw-Teitelboim gravity with matter, generalized eigenstate thermalization hypothesis, and random matrices, *Phys. Rev. D* 108 (6) (2023) 066015. [arXiv:2209.02131](https://arxiv.org/abs/2209.02131), doi:[10.1103/PhysRevD.108.066015](https://doi.org/10.1103/PhysRevD.108.066015).
- [34] G. Montavon, A. Binder, S. Lapuschkin, W. Samek, K.-R. Müller, Layer-wise relevance propagation: an overview, in: *Explainable AI: interpreting, explaining and visualizing deep learning*, Springer, 2019, pp. 193–209.
- [35] J. Craven, V. Jejjala, A. Kar, Disentangling a deep learned volume formula, *JHEP* 06 (2021) 040. [arXiv:2012.03955](https://arxiv.org/abs/2012.03955), doi:[10.1007/JHEP06\(2021\)040](https://doi.org/10.1007/JHEP06(2021)040).
- [36] W. R. Inc., [Mathematica, Version 13.3](https://www.wolfram.com/mathematica), champaign, IL, 2023. URL <https://www.wolfram.com/mathematica>
- [37] V. Jejjala, S. Mondkar, A. Mukhopadhyay, R. Raj, [ML-holo](https://arxiv.org/abs/2303.12345) (2023). URL <https://github.com/sukrut123/ML-Holo>
- [38] J. Boyd, *Chebyshev and Fourier Spectral Method*, Springer (1989). doi:[0176-5035](https://doi.org/10.1007/978-1-4613-0465-9).